Vol. 10(7), pp. 81-94, September 2018
DOI: 10.5897/JGMR2018.0296
Article Number: 774953558587
ISSN: 2006-9766

http://www.academicjournals.org/JGMR

Journal of Geology and Mining Research

Full Length Research Paper

Integrated geosciences prospecting for gold mineralization in Kwakuti, North-Central Nigeria

Ejepu J. S.*, Unuevho C. I., Ako T. A. and Abdullahi S.

Department of Geology, School of Physical Sciences, Federal University of Technology, Minna, Niger State, Nigeria.

Received 17 June, 2018; Accepted 10 August, 2018

Geoscience prospecting for gold mineralisation was conducted in Kwakuti town located within Latitudes 9.362500°N to 9.387500°N and Longitudes 6.920833°E to 6.945833°E in Northern Nigeria. The deployed geosciences techniques comprise surface geological mapping, processing and analysis of aeromagnetic total magnetic field intensity data using Oasis Montaj software and X-ray fluorescence analysis of soil samples. Migmatites and gneiss dominate the rock outcrops in the area. The migmatites occupy high elevations on the north-eastern and eastern portion of the area, where they display low magnetic field intensity values. The schist occupies moderate to low elevation areas and they display high magnetic field intensity values. The migmatites are dotted with quartz veins which constitute the gold mineralisation zone. Oval shaped high magnetic anomalous zones within the schist indicate basic intrusive into the schist. First derivative map of the magnetic field intensity data reveal NE-SW trending lineaments. They likely conducted hydrothermal fluids from the basic intrusive into the migmatites on the northeast, where gold mineralisation occurred by metasomatic ionic exchange. Spatial concentration of TiO_2 and MnO_2 are the highest within the oval shaped high magnetic anomalous zones in the southern portion of the study area. This strengthens the inference that basic intrusive underlies the area. Gold concentration distribution pattern in the area is skewed NE-SW, thereby suggesting that the NE-SW structures control the mineralisation. Mining activities will be more efficient if directed along the NE-SW structural trend.

Key words: Aeromagnetic data, aero-radiometric data, geologic mapping, gold mineralisation, X-ray fluorescence.

INTRODUCTION

With the recent priority attention given to the diversification of the Nigerian economy, the development of the solid mineral sector has become very active. The focus on how to locate and develop metalliferous deposits in the country has taken a centre stage. Gold deposit is by far the most important exploration target in the Schist belts of Nigeria and contains world class potential gold reserves. Structural and hydrothermal alterations, which are critically important in controlling gold mineralisation throughout the Schist Belts can usually, be observed directly in the magnetic and radiometric patterns (Armstrong and Rodeghiero, 2006).

*Corresponding author. E-mail: ejepu.jude@futminna.edu.ng. Tel: +2348034065079.

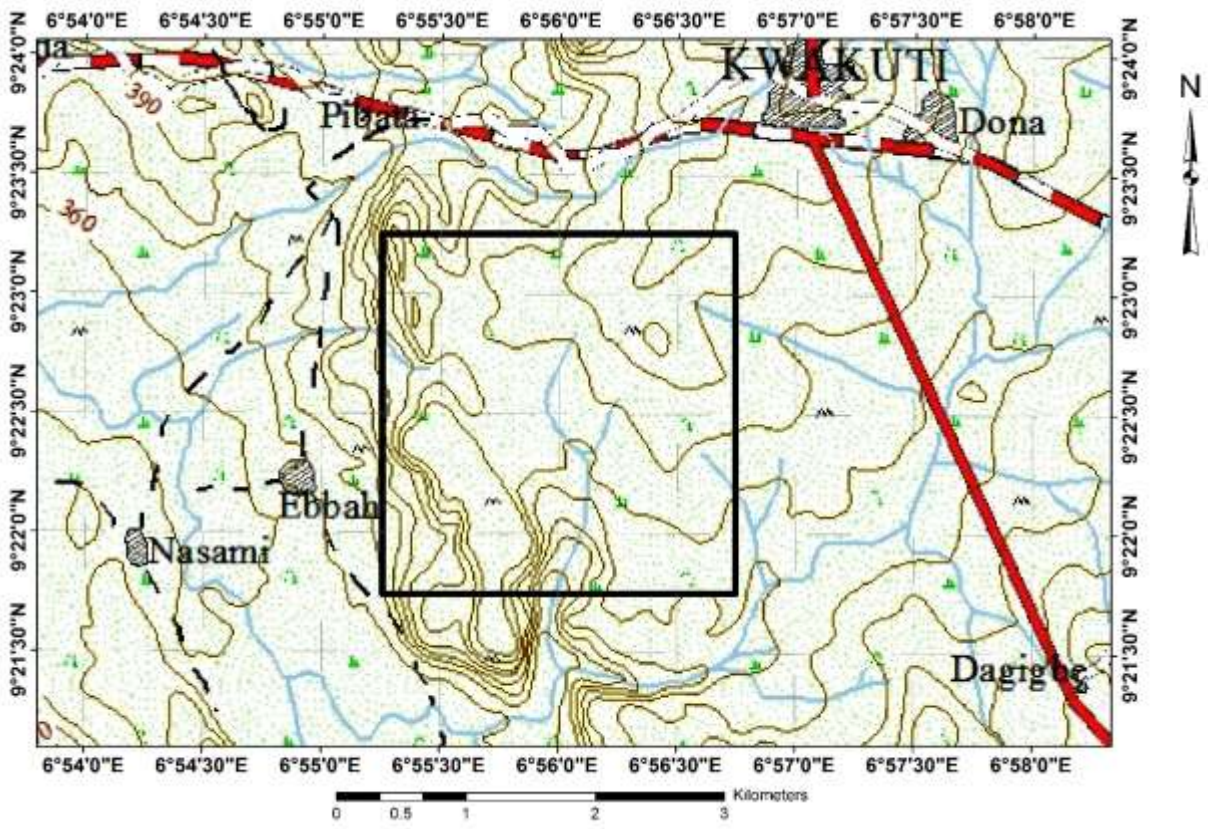

Figure 1. Topographic map showing boundary Layout of the study area.

Lithologic units, lithologic boundaries, fractures and mineral accumulations are more accurately identified and delineated using the combination of surface geological mapping, geophysical data, and geochemical data on subsurface samples. Aeromagnetic geophysical prospecting employs high magnetic susceptibility contrast between basement rocks to identify and map different lithologic units, geological structures and mineral accumulations within basement terrains (Kearey et al., 2002; Osinowo et al., 2014). The concentration of the common radioactive elements (eTh, eU and K), of the upper 30 cm of the earth's crust is measured by the radiometric method (Telford et al., 1998) and interpreting the surface by using the distribution of these radioelement, relies on the fact that rocks are made of minerals containing specific number of radio-elements. Also, the ability of surface materials to maintain valuable and detectable compositional difference between lithological units gives the efficiency of the gamma ray spectrometric method (Dickson and Scott, 1997; Wilford, 2002). Various publications have proved the usefulness of gamma ray data in mapping surface geology (Dickson and Scott, 1997; Gunn and Dentith, 1997; Graham et al., 2013). Recent improvement in the analysis of geophysical data and enhancement transforms, have increased geophysical dataset resolution, so that very insidious changes in responses can be seen (Armstrong and Rodeghiero, 2006).

Geological and geophysical interpretation of the area was carried out to gain insight into the structural setting, lithological contacts and possible alteration zones as well as identify prospective structurally controlled mineralization for subsequent ground follow-up. These surveys were aimed at producing an integrated geological and structural map that will help in delineating possible gold mineralisation zones.

Location, geomorphological and geological setting of the area

The study area lies within Latitudes 9.362500°N to 9.387500°N and Longitudes 6.920833°E to 6.945833°E of Paiko Sheet 185NE (1: 50,000 Paiko). The tenement is located in Kwakuti community (Paikoro Local Government Area of Niger State), a few kilometres off Suleja-Minna express way. The area is characterized generally by undulating geomorphology (Figure 1). There are zones of low flat terrain that are dotted with a few hills and display structurally controlled drainage of trellis pattern. The area is an integral part of schist belt that hosts gold mineralization in Nigeria. The dominant rocks are the

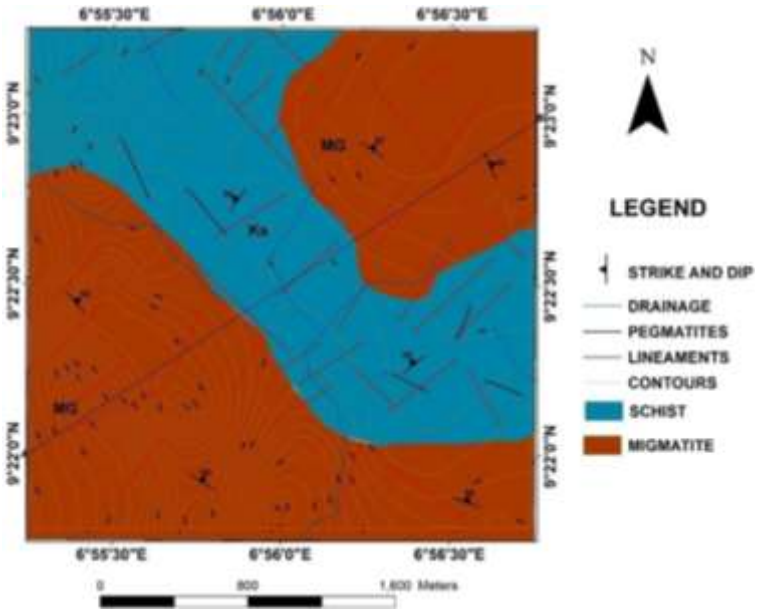

Figure 2. Geologic map of the study area. Some fault lines are digitized from published geologic map. (Source: Nigerian Geological Survey Agency (NGSA), 2009).

migmatites and schist. Pegmatite dykes occur within the schist while the migmatites outcrop over larger surface area than the schist. Feldspar, quartz and muscovite are major constituents within the schist. All the outcropping lithologic units in the area are transverse by quartz veins. The area is highly mineralized with gold occurring within pegmatite schist, quartz veins and in alluvium.

The structural elements in the study area include joints, faults, foliations and minor folds. The migmatites and schist generally trend NE-SW. The quartz veins are found trending NE-SW and in some areas. The quartz veins are seen to be of great importance in the present study because they host their cases of gold infillings within them. Most of these structural elements do not appear on the map due to the scale of the map. Dolerite dykes are seen cutting across some of the outcrops. Fracturing may be as a result of thermo tectonic deformational events mostly of the Eburnean and Pan-African Orogeny (Oluyide, 1988) (Figure 2). The dominant NE-SW structural trend coheres with the tectonic grain of the schist belt (Olasehinde et al., 2013; Ejepu et al., 2015).

METHODOLOGY

Primary mineralization in Nigeria is mostly lithologically and structurally controlled (Ajakaiye et al., 1991). Structures include faults, shear zones (lineaments), pegmatites, quartz and quartzite veins. The methodology for this study was therefore structured to capture the general trends of surface and subsurface structures which control primary gold mineralization in the area. The exercise comprised surface geological mapping, lithologic and structural analysis of remote sensing images, pitting and sample collection. Soil samples were collected in the neighbourhood of stream channels and analysed using X-ray fluorescence.

Geologic mapping

Geological mapping exercise was carried out by locating areas of good outcrop exposures. Mapping was done using a topographic map on a scale of 12,500. Areas of geological interest were studied and tracked with the aid of a GPS device. Captured spatial data were tied to UTM, WGS 84 Zone 32N system.

Aeromagnetic data processing and interpretation

The aeromagnetic data was obtained from Nigeria Geological Survey Agency (NGSA). The data was acquired along a series of NE-SW tie lines direction with a flight line spacing of 500 m and terrain clearance of 80 m. The average magnetic inclination and declination across the survey is -5.49 and -1.99°, respectively. The data was gridded using the minimum curvature gridding method (Briggs, 1974) using ArcGIS software. The magnetic data was initially subjected to reduction to the magnetic equator (RTE) and was further processed to investigate the presence of buried structures that might be relevant in the mineral exploration study. Directional and normalised derivatives were calculated to accentuate near surface structures from which lineaments were identified and delineated. These include first vertical, total horizontal and tilt derivatives analytic signal. Source parameter imaging algorithm was applied to the RTE magnetic data to model depth to causative bodies.

Due to the inherent problem of low latitude anomaly shift, the magnetic grid was reduced to the equator and then inverted. This was done with the aim of making magnetic anomalies to centre on their respective causative bodies. MAGMAP was used to calculate the first vertical derivative of the magnetic data. This enhancement

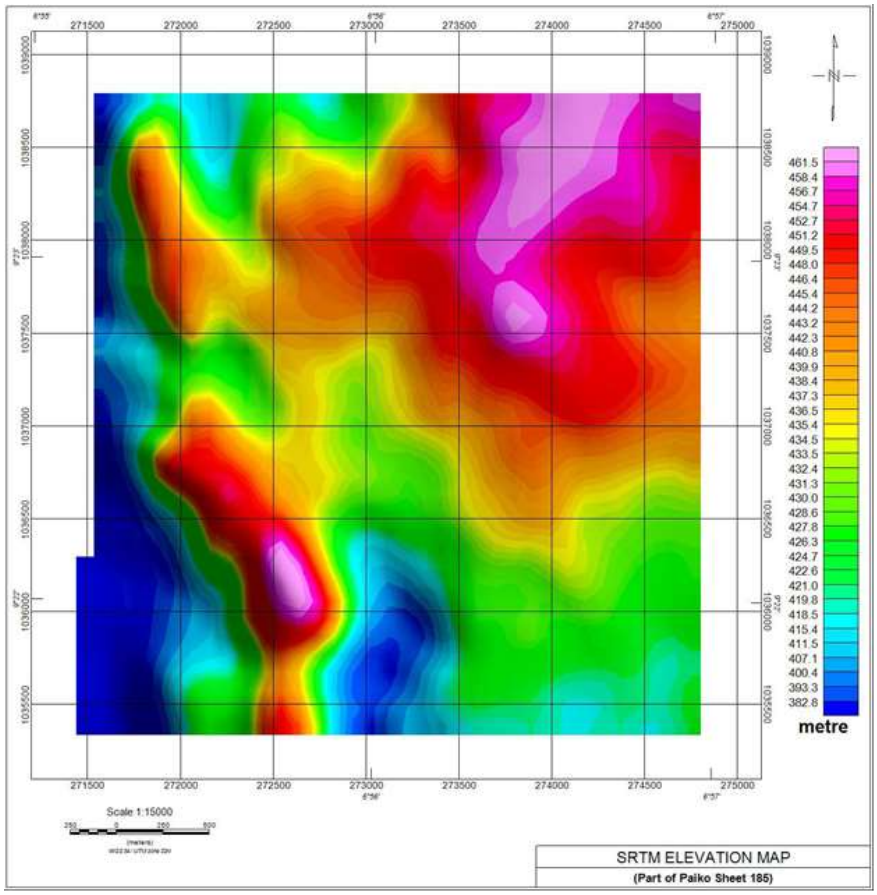

Figure 3. SRTM elevation map.

sharpens up anomalies over bodies and tends to reduce anomaly complexity, allowing a clearer imaging of the causative structures. The transformation can be noisy since it will amplify short wavelength noise.

The total horizontal derivative and the tilt derivative are both useful in mapping shallow to near surface basement structures. These enhancements are also designed to image faults and contact features. They complement the results of the vertical derivative processing. The analytic signal processing generates a maximum directly over discrete magnetic bodies, as well as over their edges. The width of a maximum, or ridge, is an indicator of the depth to the contact. This transformation is often useful at low magnetic latitudes because of the inherent problems with reduction to the pole (RTP) at such low latitudes (Geosoft Inc., 2014).

Radiometric data processing and interpretation

Gamma-ray spectrometry (GRS) can be very helpful in mapping surface geology. The method provides estimates of apparent surface concentrations of the most common naturally occurring radioactive elements comprising potassium (K), equivalent uranium (eU), and equivalent thorium (eTh). The use of the method for geological mapping is based on the assumption that absolute and relative concentrations of these radio elements vary measurably and significantly with lithology.

The radioelement composite image presents a single display of the three radioelement concentrations. This map suggests to a great extent the lithological differences due to the variations in colour. The Uranium (U), Thorium (Th) and Potassium (K) ternary map emphasize regions where the specific radioelement has a total and pretty higher amount (Elawadi et al., 2004) using ratios of the three bands with K assigned to red, U to blue and Th to green.

Pitting and geochemical analysis

Locations for pitting were chosen from analysis of aeromagnetic map. Seven pits were dug to ascertain spatial extent of subsurface mineral occurrence. This was aimed at delineating or establishing a target size with better mineralization. Stream sediments were collected based on the anomalous regions from the geophysical surveys. The site for the sampling coincided in drainage channels and samples were taken at about 0.3 m from the surface the stream.

RESULTS AND DISCUSSION

Field investigations

Figure 3 shows is a digital elevation model of the study area. It reveals high elevation regions on the north-eastern and eastern portions of the area. Low elevation

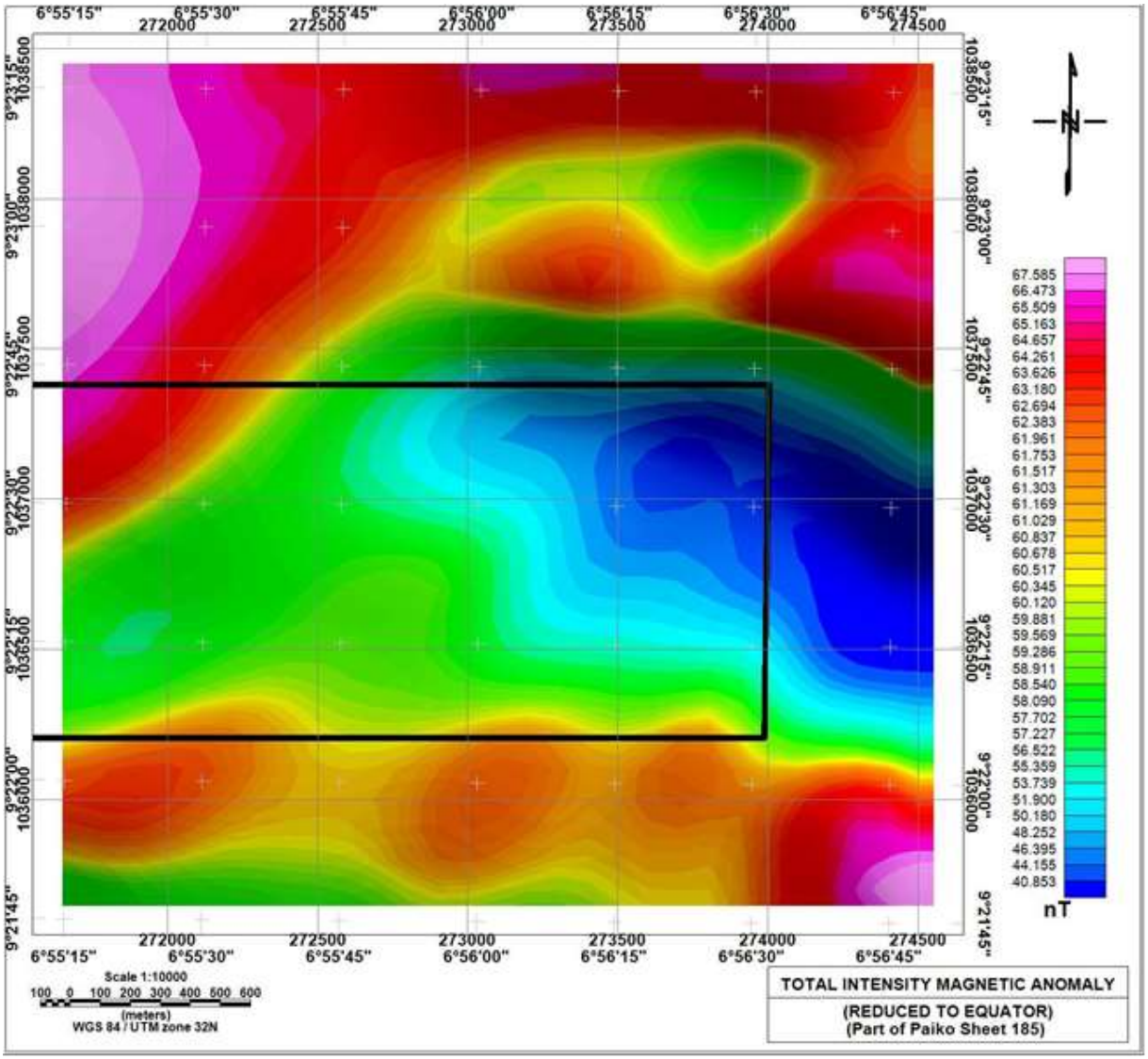

Figure 4. Reduce-to-Equator total intensity magnetic anomaly map. Map was produced using Geosoft Oasis montaj. Black outline represents coverage where samples were taken for geochemical analysis.

regions dominate the south-western and western portions.

Geophysical data processing and interpretation

Figure 4 shows the reduced to equator (RTE) map generated from the total intensity magnetic anomaly (TIMA) data for the study area. The blocked region is the region covered by Shuttle Radar Topography Mission (SRTM) elevation map of Figure 3. The map reveals that magnetic field intensity values that range from 40 to 67 nT characterise the rocks in the study area. The high elevations regions (Figure 3) coincide with very low magnetic regions (Figure 4) and are underlain with migmatites and dykes. Areas of moderate elevation are associated with high magnetic anomaly corresponding to schistose rocks. Contact zones recorded low magnetic anomaly. This is an indication of demagnetization of magnetite minerals to hematite minerals with low magnetic response as a result of hydrothermal fluid flow through fractures and faults (Wilford et al., 1997). This is as a result of severe shearing and faulting at the contact zones. This prospective fault-bounded contact between the schists and the migmatites may potentially hosts mineralization zones in the area.

First vertical derivative (FVD)

The FVD map (Figure 5) helped attenuate broad, more regional anomalies and enhanced local, more delicate

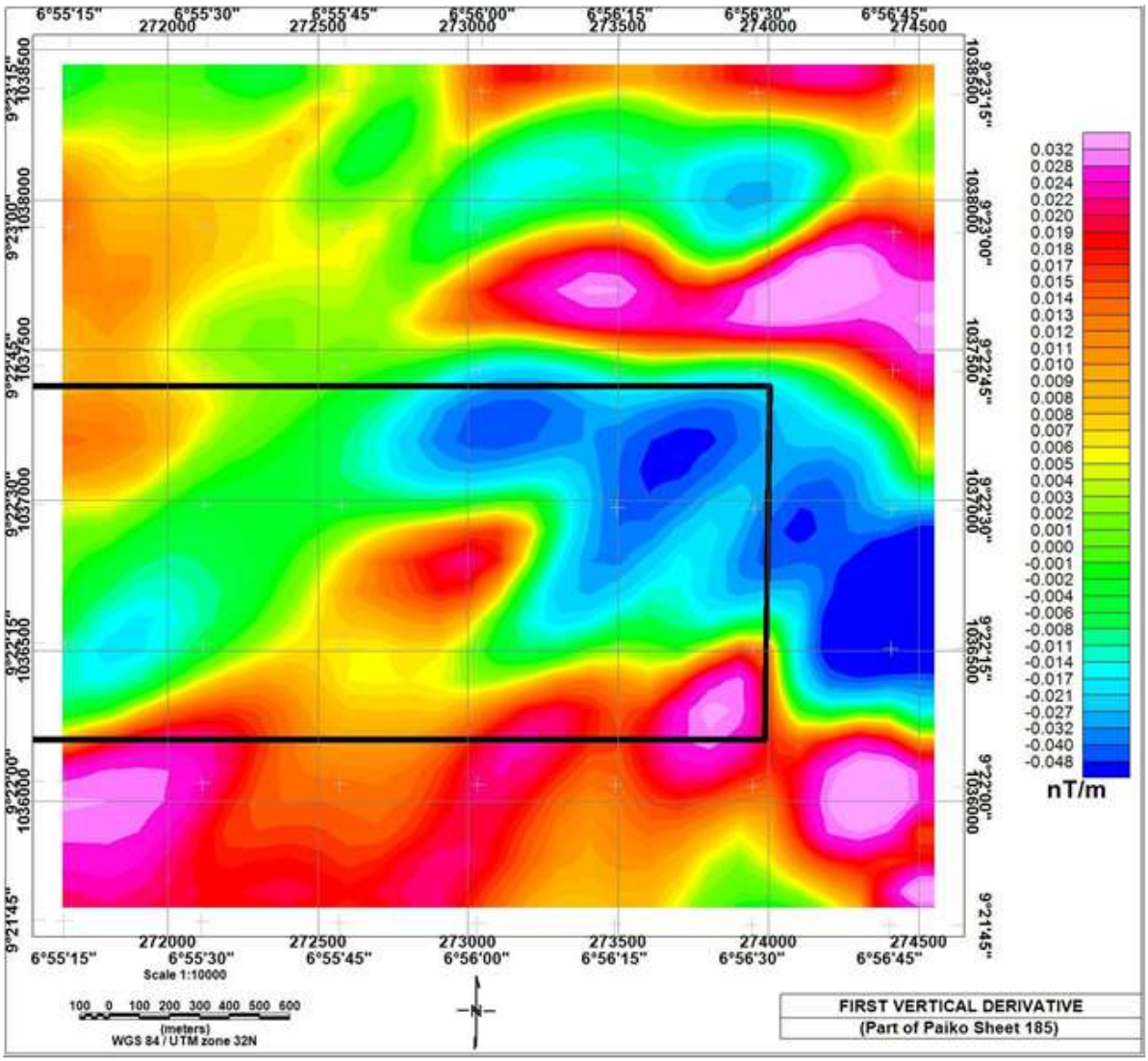

Figure 5. First vertical derivative (FVD) map. Map was produced using Geosoft Oasis montaj. Black outline represents coverage where samples were taken for geochemical analysis.

magnetic responses because of their sensitive to shallow magnetic source bodies and contacts. It reveals NE-SW and NW-SE trending lineaments. Oval shaped anomalies with high total magnetic intensity values in the southern portion of Figure 5 may indicate basic intrusives into the schist. The quartz veins are hosted mainly in migmatites and are closely associated with the gold mineralization. The NE-SW trending lineaments are likely fractures that conducted hydrothermal fluids from basic intrusive into migmatites on the northeast.

Tilt derivative map (TDR)

Applying the tilt derivative highlighted signatures of shallow magnetic sources and so gave some guidance on interpreting known lineaments and zones. The TDR map (Figure 6) enhanced weak magnetic anomalies, otherwise overshadowed by stronger structures in the area improving subtle fabric. The NE-SW trending lineaments are also revealed in the TDR map; the map also reveals NW-SE trending lineaments on its north-eastern portion. Both lineaments constitute a conjugate fracture system. Since the NE-SW trending lineaments run through the schist and migmatites, they seem to control the mineralisation in the area.

Analytic signal (AS)

The analytic signal map (Figure 7) produced maxima directly over discrete bodies and their edges. The width

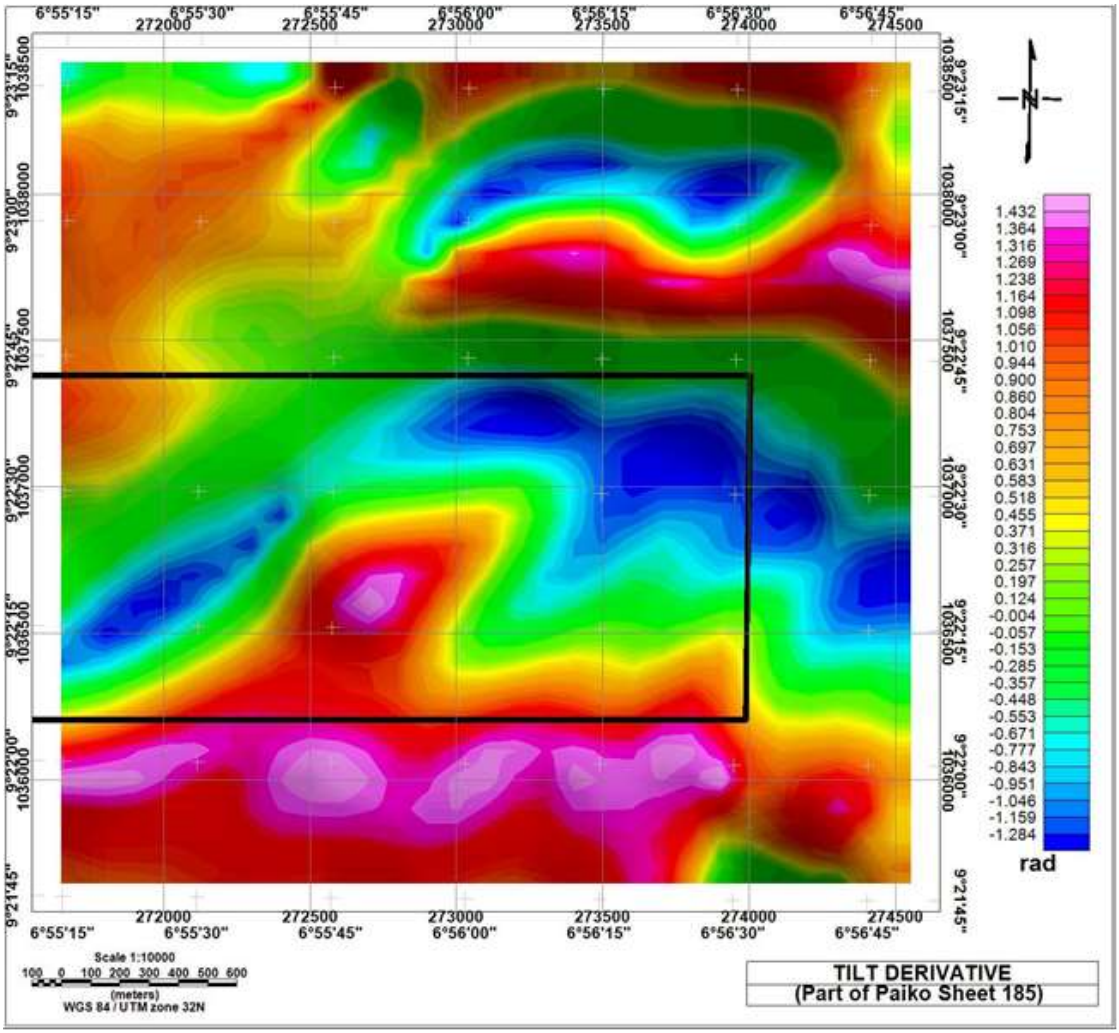

Figure 6. Tilt Derivative map. Map was produced using Geosoft Oasis montaj. Black outline represents coverage where samples were taken for geochemical analysis.

of the maxima is indicative of the depth of the body (MacLeod et al., 1993). The NW-SE trending lineaments are indicated on the AS map. It also revealed high magnetic anomaly zones in the north-eastern portion. Schist showed low magnetic anomalies as it should with values between 0.006 nT/km and 0.020 nT/m, indicated mostly by blue and green colour at the central part. The migmatites showed high magnetic anomaly fringes with values up to 0.081 nT/m indicated by red/magenta to green colours.

Figure 8 shows a map displaying the composite lineaments obtained from the different processing of the total magnetic field intensity data and the lineaments determined from surface geological mapping exercise. The dominant lineaments are the conjugate NW-SE and NE-SW fractures. Major trend in the NE-SW direction, some trend in the NW-SE direction. These structures interpreted from the derivative aeromagnetic maps are essential channels for mineralization fluids. The NE-SW trends represent the mega shear zones in Africa called the Central African Shear Zone (CASZ) which resulted from the important tectonic movements that occurred during the Pan-African orogenic cycle (Moreaus et al., 1987). It is also a dextral shear zone that is related to the wider mylonite belts pre-dating at the cretaceous times, the opening of the South Atlantic Ocean (Djomani et al., 1995). Correlation between interpreted lineaments in relation to gold mineralisation shows significant spatial relationship. This has demonstrated that the data used in the study has proven to be useful in identifying known and new geologic features in the area especially when they are integrated.

Ternary image

The ternary image (Figure 9) presents strong spatial correlations with the known geologic units and the most

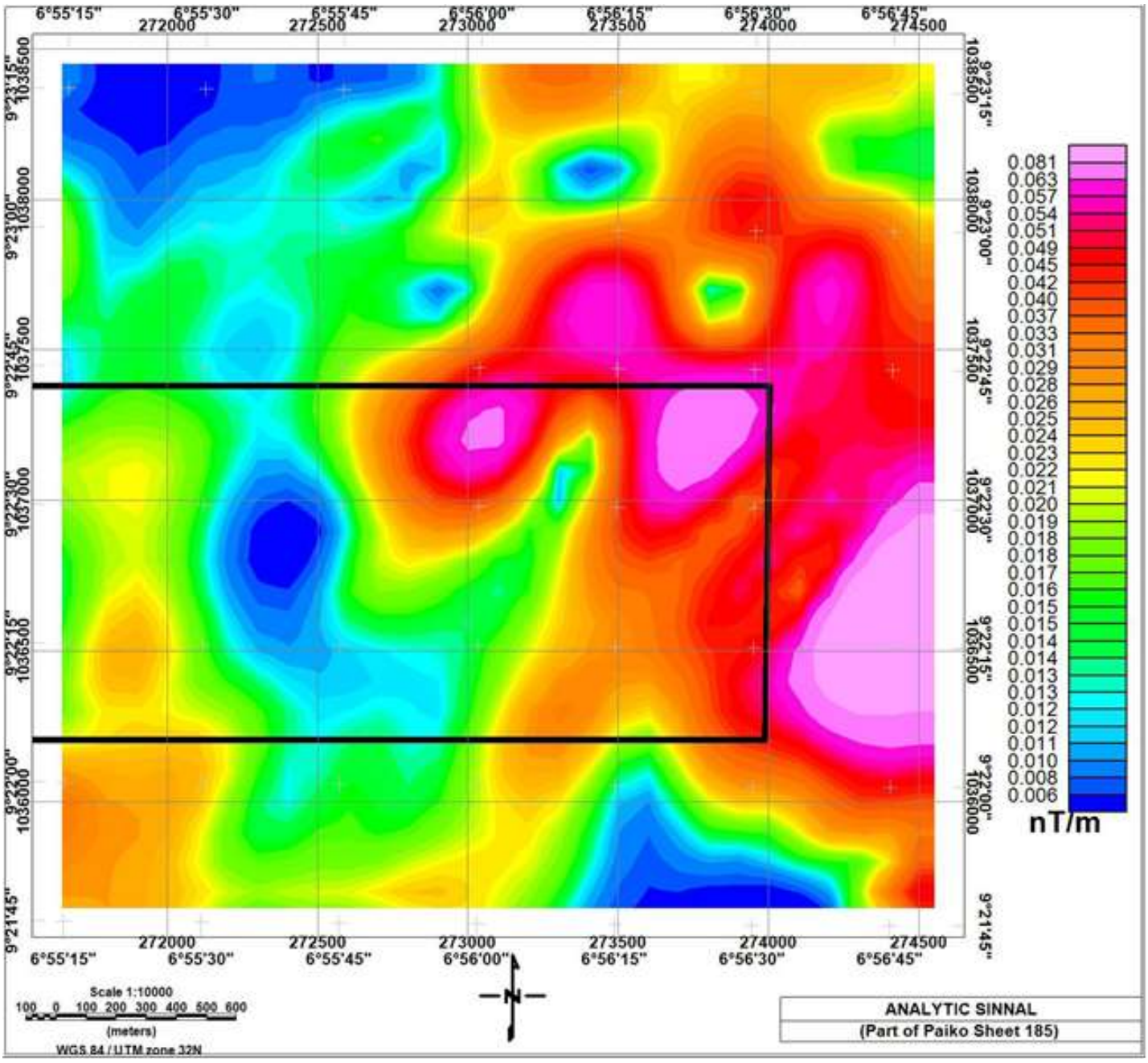

Figure 7. Analytic signal map. Map was produced using Geosoft Oasis montaj. Black outline represents coverage where samples were taken for geochemical analysis.

prominent features in the K, Th, and U images. The most notable units in the ternary image are the mafic and magnetite rich migmatite formations which are represented in cyan and also notable in both U and Th maps. In addition, the migmatite with high K concentration and some traces of U are given a magenta colour. This strong correlation is based on the fact that the migmatite are made up of the potash-rich (high K concentration) regolith which comes in the form of muscovite and biotite as well as the mineral constituents of the pegmatite dykes (Wilford et al., 1997).

The K, Th and U map show that the schist recorded weak anomaly of K and Th but strong U anomaly. A long denudation period of weathering has probably depleted most of the U concentration of migmatites within the western portion of the ternary map. The dark regions which occur within faulted zones and in some areas at the contact zones of the rock formation can be attributed

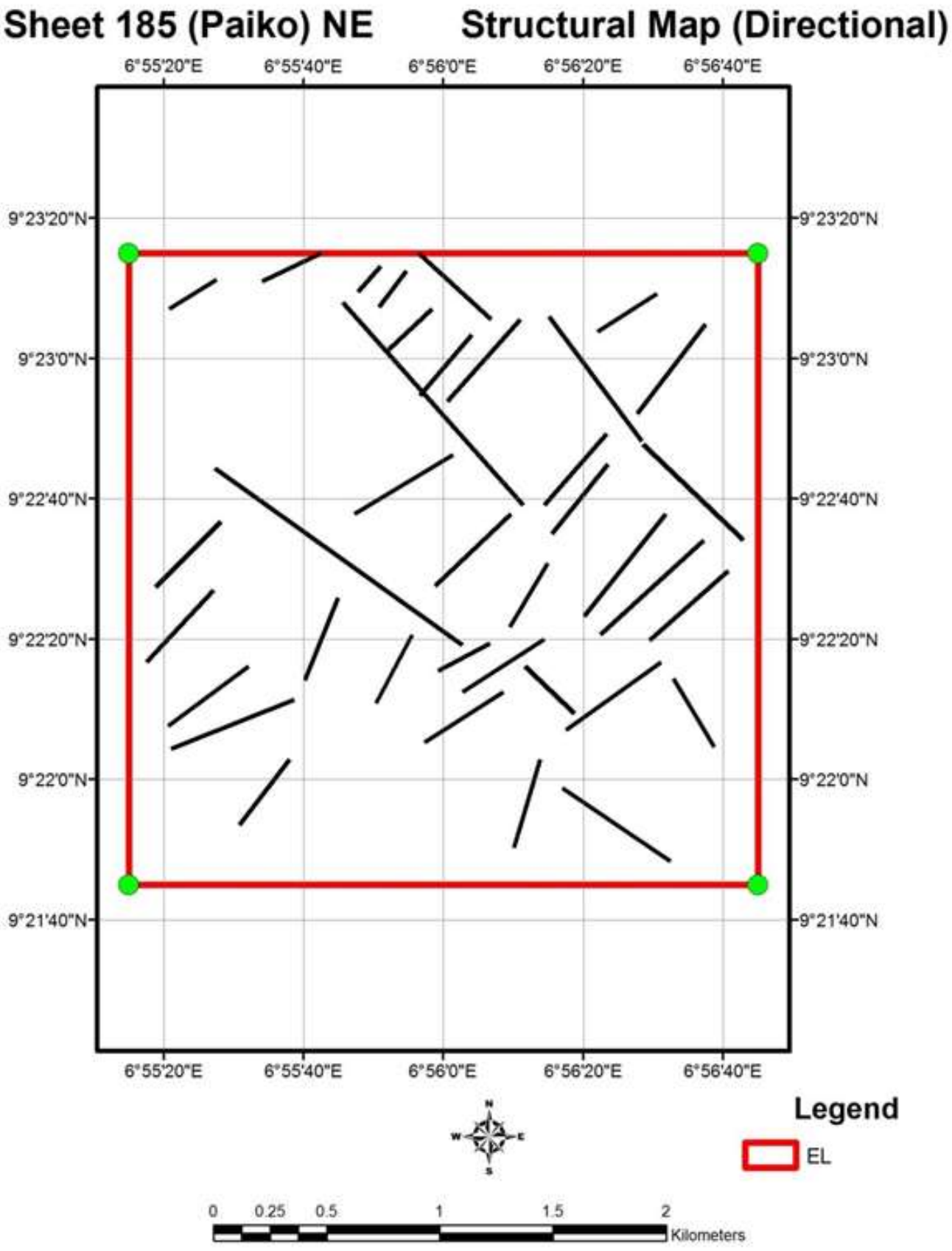

Figure 8. Lineament map of the study area. Some mapped surface structures are also represented.

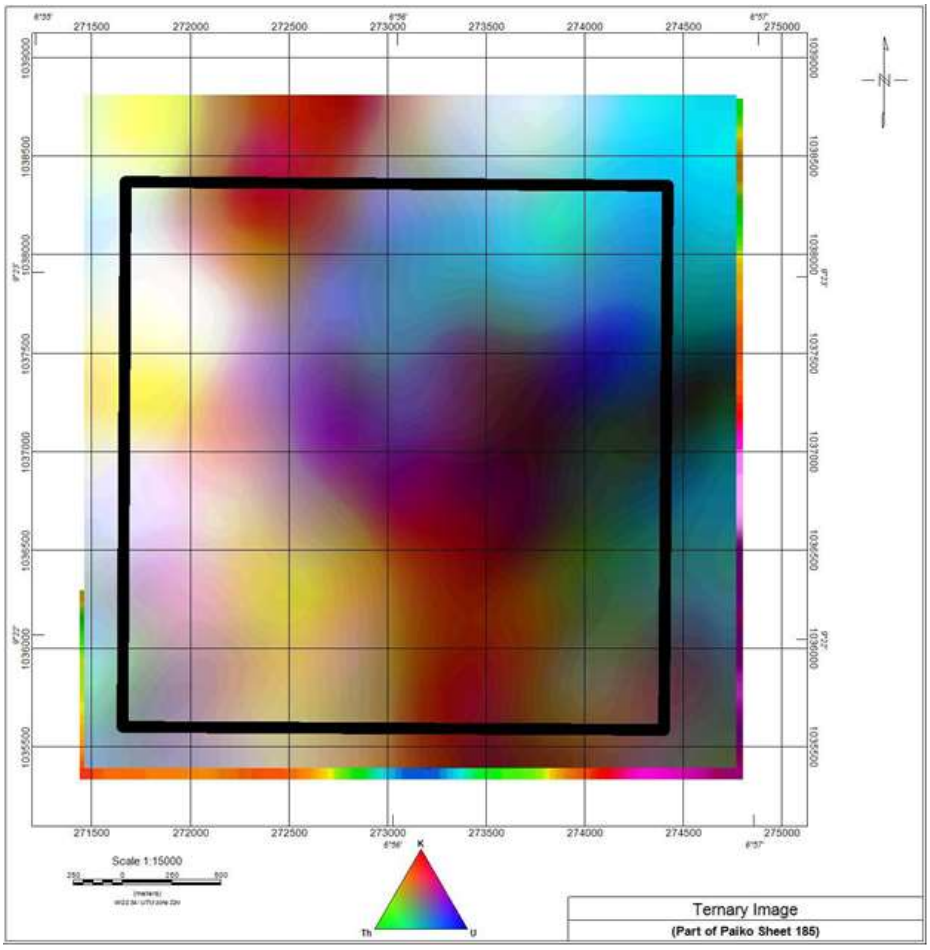

Figure 9. Ternary Image Map produced from equivalent potassium, thorium and uranium concentrations. Map was produced using Geosoft Oasis montaj.

Table 1. Geographic coordinates of the pits.

Pit number	Longitude (E)	Latitude (N)
01	6°56'03.0"	9°22'05.3"
02	6°55'23.7"	9°22'11.9"
03	6°55'09.3"	9°22'24.4"
04	6°55'16.8"	9°22'33.4"
05	6°55'26.3"	9°22'40.4"
06	6°55'34.9"	9°22'37.2"
07	6°56'31.6"	9°22'43.3"

to the low concentration of the K, Th and U. The light-yellow zones in the ternary image are indications of high concentration of K, Th, but low U concentrations.

Pitting and geochemical analyses

The geographic coordinates of the sampled pits are shown in Table 1; the concentration of the major oxides in percentage is show in Table 2 and determined trace elements and rare earth elements are shown in Table 3. The geochemical composition of stream sediments obtained with X-ray fluorescence method of analysis is shown in Tables 2 and 3. The stream sediments are made up of considerably high percentage of silica ranging from 48 to about 70 wt%. The composition of

Table 2. Major oxides (%).

Sample ID	SiO_2 (%)	Al_2O_3 (%)	SO_3 (%)	P_2O_5 (%)	Na_2O (%)	K_2O (%)	CaO (%)	MgO (%)	TiO_2 (%)	Fe_2O_3 (%)	MnO (%)	H_2O (%)
LOC. 1	54.20	14.08	-	-	1.04	8.26	1.20	0.24	4.83	10.40	0.06	5.68
LOC. 2	69.80	8.41	-	-	0.02	2.40	4.95	0.54	6.22	5.12	0.22	2.30
LOC. 3	48.10	19.00	-	-	0.41	4.24	0.78	-	1.86	18.10	0.16	7.33
LOC. 4	65.80	7.98	-	-	0.32	2.70	2.89	1.04	2.84	10.42	0.075	5.93
LOC. 5	59.70	18.00	-	-	1.02	5.51	0.47	-	2.55	7.99	0.035	4.72
LOC. 6	60.00	13.21	-	-	1.04	7.09	1.68	0.02	1.68	9.00	0.12	6.14
LOC. 7	56.20	18.34	-	-	1.54	5.34	1.90	0.03	3.03	8.84	0.14	4.60

Table 3. Trace elements/rare earth metals (ppm).

Element (ppm)	LOC. 1	LOC. 2	LOC. 3	LOC.4	LOC. 5	LOC. 6	LOC. 7
Ag	3.040	1.606	3.346	1.354	1.628	2.252	1.790
As	0.008	<0.001	5.001	<0.001	0.900	<0.001	<0.001
Au	2.940	0.872	3.588	2.018	2.620	0.296	1.954
Bi	1.240	2.140	1.483	3.025	3.312	0.895	0.864
Cd	<0.001	<0.001	<0.001	<0.001	<0.001	<0.001	<0.001
Ce	<0.001	<0.001	<0.001	<0.001	<0.001	<0.001	<0.001
Co	<0.001	<0.001	<0.001	<0.001	<0.001	<0.001	<0.001
Cr	0.880	0.083	0.630	2.400	1.420	0.635	0.782
Cs	<0.001	<0.001	<0.001	<0.001	<0.001	<0.001	<0.001
Cu	0.100	0.130	0.220	0.044	0.120	0.053	0.055
Eu	0.480	0.540	0.530	0.170	0.200	0.230	0.420
Ga	0.010	<0.001	4.001	<0.001	<0.001	0.801	<0.001
Ge	<0.001	<0.001	<0.001	<0.001	<0.001	<0.001	<0.001
Mo	<0.001	<0.001	<0.001	<0.001	<0.001	<0.001	<0.001
Nb	<0.001	<0.001	<0.001	<0.001	<0.001	<0.001	<0.001
Ni	<0.001	<0.001	<0.001	<0.001	<0.001	<0.001	<0.001
Os	<0.001	<0.001	<0.001	<0.001	<0.001	<0.001	<0.001
Pb	0.180	0.084	10.087	<0.001	0.690	<0.001	<0.001
Re	0.100	0.070	0.200	0.700	0.042	0.130	0.120
Sr	0.018	0.110	0.140	0.290	<0.001	0.970	0.010
Ta	<0.001	<0.001	<0.001	<0.001	<0.001	<0.001	<0.001
Th	<0.001	<0.001	<0.001	<0.001	<0.001	<0.001	<0.001
Tl	<0.001	<0.001	<0.001	<0.001	<0.001	<0.001	<0.001
U	<0.001	<0.001	<0.001	<0.001	<0.001	<0.001	<0.001
V	0.702	0.512	<0.001	0.680	0.730	0.850	0.500
W	<0.001	<0.001	<0.001	<0.001	<0.001	<0.001	<0.001
Zn	0.840	1.470	0.180	2.000	1.700	0.370	1.002
Zr	48.00	25.000	6.500	1.200	1.770	0.288	0.2985

Al_2O_3 varies from 7.98 to 19.00 wt%, Fe_2O_3 ranges from 5 to 18.00 wt%. The concentrations of other major oxides are relatively very low. Zirconium (Zr) has the highest concentration of 48 ppm. This is followed closely by Ag and Au with 3.04 and 2.94 ppm. It is noteworthy that only the first pit contains these anomalously high concentrations of these elements. Zr, a correlation on the various oxides and elements does not show somewhat weak spatial relationship.

However, spatial distribution of TiO_2 and MnO_2 (Figures 10 and 11), respectively reveals the highest concentration of these oxides in the south-western portion of the area. This supports the interpretation that oval shaped high anomalies in the FVD map (Figure 5)

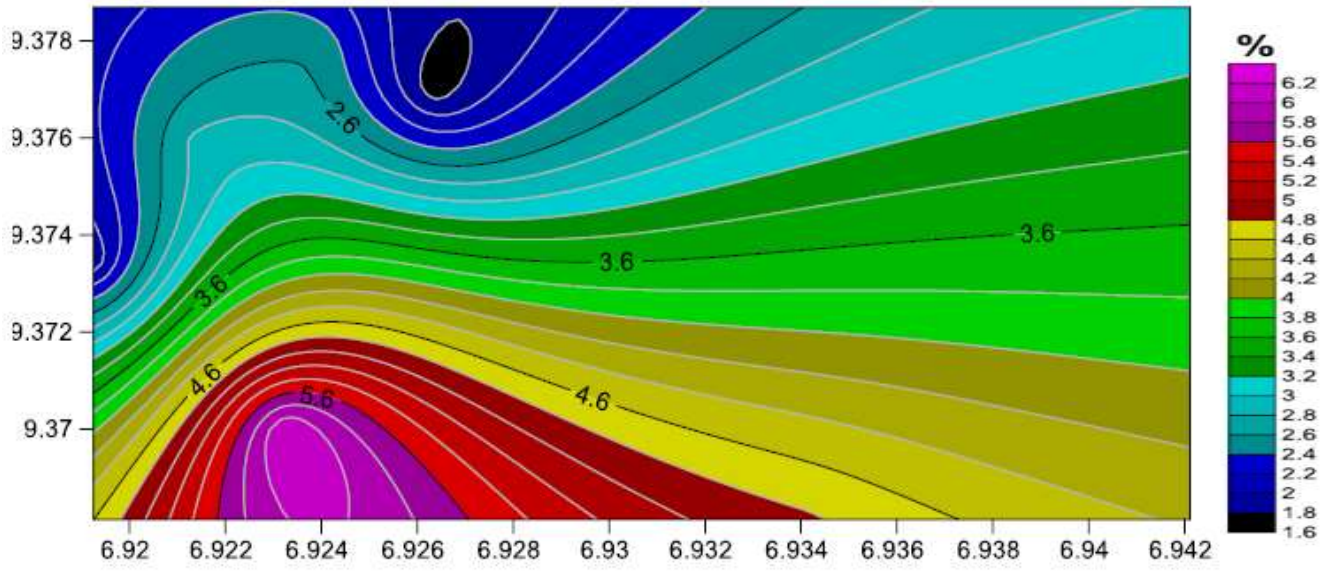

Figure 10. Contour plot of geochemical distribution of TiO_2 (%) for pit samples in the area.

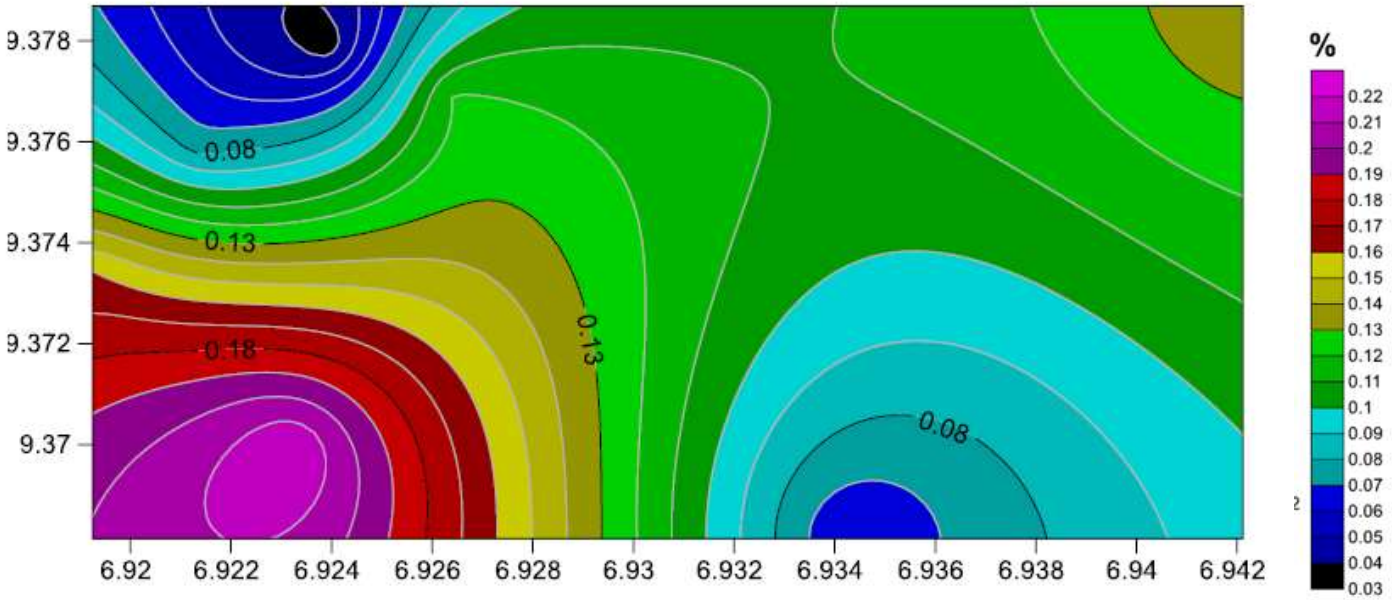

Figure 11. Contour plot of geochemical distribution of MnO (%) for pit samples in the area.

are basic intrusive. Figure 12 which shows the spatial distribution of gold concentrations with the highest concentration of about 3.6 ppm in the north-western portion of the map, have NW-SE alignment of the concentration pattern. This however does not support the interpretation that the NE-SW fractures conduct hydrothermal fluids from basic intrusive in the southwestern portion to migmatites in the north-eastern portion of the study area. This is also a reason to believe that the concentrations of these elements show no spatial relationship.

CONCLUSION AND RECOMMENDATION

The work presented a new integrated geological, aeromagnetic and aero-radiometric dataset for structural interpretation of the area through mapping the lithology, geological structures, lineaments and hydrothermal alteration zones associated with possible gold

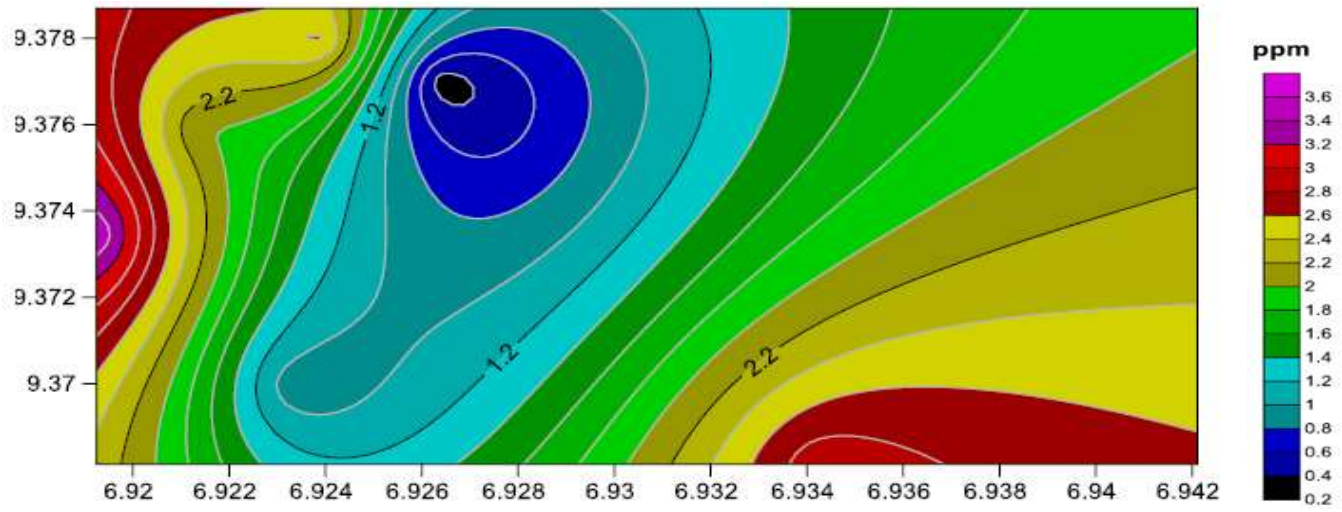

Figure 12. Contour plot of geochemical distribution of Au (ppm) for pit samples in the area.

mineralisation zones. This was achieved by enhanced images such as total magnetic intensity, analytical signal, horizontal derivative, vertical derivative and ternary radiometric maps.

Using observations from the enhanced airborne magnetic and radiometric maps, it has been established that the area has undergone a pronounced tectonic activity resulting in shearing and fracturing. A common feature of gold mineralization in Nigeria is their close proximity to major and subsidiary fault structures. So, the sheared zone and fractures are potential channels for mineralization fluids. The observed zonation in the magnetic data and the potassic alteration in the ternary image are indication of hydrothermal alteration associated with mineralization. Often this alteration signature may be broad and laterally extensive providing a larger exploration target. The contacts between different geological units, the intersections between linear features, sheared and fractured zones are potential traps for gold mineralization and therefore give a significant exploration vector.

The locations of core drilling for further exploration efforts shall be based on recommended sites from the more detailed ground geophysical and geochemical surveys. Fire assay geochemical analysis is preferred for soil and selected rock samples that have been taken from various anomalous regions in the prospect area.

CONFLICT OF INTERESTS

The authors have not declared any conflict of interests.

REFERENCES

Ajakaiye DE, Hall DH, Ashiekaa JA, Udensi EE (1991). Magnetic anomalies in the Nigerian continental mass based on aeromagnetic surveys. Tectonophysics 192(1):211-230.

Armstrong M, Rodeghiero A (2006). Airborne Geophysical Techniques in Aziz. Coal Operators' Conference, University of Wollongong and the Australasian Institute of Mining and Metallurgy pp. 113-131.

Briggs IC (1974). Machine contouring using minimum curvature. Geophysics 39(1):39-48.

Dickson BL, Scott KM (1997). Interpretation of aerial gamma-ray surveys - Adding the geochemical factors. Journal of Australian Geology and Geophysics 17:187-200.

Djomani YHP, Nnange JM, Diament M, Ebinger CJ, Fairhead JD (1995). Effective elastic thickness and crustal thickness variations in west central Africa inferred from gravity data. Journal of Geophysical Research 100:22047-22070.

Ejepu SJ, Olasehinde PI, Omar DM, Abdullahi DS, Adebowale TA, Ochimana A (2015). Integration of geology, remote sensing and geographic information system in assessing groundwater potential of Paiko Sheet 185 north-central Nigeria. Journal of Information, Education, Science and Technology 2(1):145-155.

Elawadi E, Ammar A, Elsirafy A (2004). Mapping surface geology using airborne gamma ray spectrometric survey data - A case study. Proceedings of SEGJ international symposium. Nuclear Materials Authority of Egypt, Airborne Exploration Department.

Geosoft Inc. (2014). GM-SYS Gravity and Magnetic Modelling Software, Users Guide, v.4.10, Northwest Geophysical Associates, Inc., P.O. Box 1063, Corvallis, Oregon 97339-1063 USA, 2006.

Gunn P, Dentith M (1997). Interpreting aeromagnetic data in areas of limited outcrop. AGSO Journal of Geology and Geophysics 17(2):175-185.

Graham K, Wemegah D, Preko K (2013). Geological and structural interpretation of part of the Buem formation, Ghana, using aerogeophysical data. Master's thesis, Department of Physics, Kwame Nkrumah University of Science and Technology.

Kearey P, Brooks M, Hill I (2002). An introduction to geophysical exploration, John Wiley and Sons. Keating PB (1995). A simple technique to identify magnetic anomalies due to Kimberlite pipes. Exploration and Mining Geology 4:121-125.

MacLeod IN, Jones K, Dai TF (1993). 3-d analytic signal in the interpretation of total magnetic field data at low magnetic latitudes. Exploration Geophysics 24: 679-687.

Moreaus C, Reynoult JM, Deruelle B, Robineau B (1987). A new tectonic model for the Cameroon Line, Central Africa. Tectonophysics 139:317-334.

Nigerian Geological Survey Agency (NGSA). (2009). http://ngsa.gov.ng/.

Olasehinde PI, Ejepu SJ, Alabi AA (2013). Fracture Detection in a hard rock terrain using radial geoelectric sounding techniques. Water Resources Journal 23(1 and 2):1-19.

Oluyide PO (1988). Structural trends in the Nigerian Basement Complex. In: Precambrian Geology of Nigeria. Geological Survey of Nigeria, Kaduna pp. 93-98.
Osinowo OO, Akanji AO, Olayinka AI (2014). Application of high resolution aeromagnetic data for basement topography mapping of Siluko and environs, south-western Nigeria. Journal of African Earth Sciences 99:637-651.
Reynolds RL, Rosenbaum JG, Hudson MR, Fishman NS (1990). Rock magnetism, the distribution of magnetic minerals in the earth's crust and aeromagnetic anomalies. US Geological Survey Bulletin 1924:24-45.
Telford WM, Geldart LP, Sheriff RE (1998). Applied Geophysics (2nd Ed.), Springer, Berlin 770 p.
Wilford JR, Bierwirth PN, Craig MA (1997). Application of airborne gamma-ray spectrometry in soil/regolith mapping and applied geomorphology. AGSO Journal of Australian Geology and Geophysics 17:201-216.
Wilford J (2002). Airborne gamma-ray spectrometry. Cooperative Research Centre for Landscape Environments and Mineral Exploration. Commonwealth Scientific and Industrial Research Organization 144:46-52.